Science Advances

Supplementary Materials for

Agriculture is a major source of NO$_x$ pollution in California

Maya Almaraz, Edith Bai, Chao Wang, Justin Trousdell, Stephen Conley, Ian Faloona,
Benjamin Z. Houlton

This PDF file includes:

- Supplementary Methods
- table S1. Crop classification and fertilizer rate data (mean for 1964 to 2006) collected from the DWR of California and USDA fertilizer consumption database.
- table S2. ABL heights, z_i, and budget terms for the six flights.
- table S3. NO$_x$ budget table and the consequent total regional emissions for each flight.
- table S4. Flight estimates of total NO$_x$ and soil NO$_x$ and model estimates of soil NO$_x$ for the flight area in fig. S3 [Coordinates box: (36º51′52.09″N, 120º43′19.65″W), (37º0′6.85″ N, 119º50′53.87″W), (35º57′49.03″N, 120º1′37.93″W), and (36º5′27.03″N, 118º58′2.91″W) compared with CARB inventory of total NO$_x$].
- fig. S1. Model of how nitrogen oxide (NO), nitrous oxide (N$_2$O), and dinitrogen (N$_2$) partitioning varies with water-filled pore space.
- fig. S2. Sensitivity of NO emission from croplands to different input parameters: soil organic carbon (fsoc), soil texture (ftxt), soil drainage (fdrain), and climate (fclim).
- fig. S3. Airborne NO$_x$ observation sampling area.
- References (*55–58*)

Supplementary Methods

Land cover. The land cover was divided into five major classes: crops, wetland rice, grassland, pastoral system, and natural system. The crops were further divided into 67 types of crops (table S1).

Estimation of regional NO$_x$ emissions from in-situ aircraft data. The budget equation for ABL-averaged nitrogen oxides concentration, [NO$_x$], can be written as

$$\frac{\partial [NO_x]}{\partial t} = \frac{F_0 + w_e \Delta [NO_x]}{z_i} - \frac{[NO_x]}{\tau_{NOx}} - U \frac{\partial [NO_x]}{\partial x}$$

where the terms are (left to right): the observed time rate of change (sometimes referred to as 'storage'), net vertical mixing across the ABL boundaries (the difference between the surface flux, F_0, and the entrainment flux at z_i, the top of the ABL, which is parameterized as $-w_e \Delta [NO_x]$), photochemical loss (due to oxidation of NO$_2$ to nitric acid by OH, represented here as a chemical loss time scale, τ_{NOx}), and advection by the horizontal wind (the influence of the mean wind on the large scale horizontal gradient, here the x direction is rotated such that there is no mean crosswind component). The entrainment velocity, w_e, represents the rate at which the ABL incorporates overlying air (usually less polluted) during its growing phase during the daytime, and its estimate is discussed below.

The data used for the budgets was collected between about 11:15 to 15:00 PST during six flights (27-29 July and 4-6 August, 2016) between Fresno and Visalia when the atmospheric boundary

layer was growing progressively after its initial rapid growth phase through the residual layer in the mid-morning. The flights were performed as part of the California Baseline Ozone Transport Study (CABOTS) under the auspices of the California Air Resources Board (CARB), and the data can be accessed here (https://www.esrl.noaa.gov/csd/groups/csd3/measurements/cabots/). ABL growth is diagnosed by periodic vertical profiles of the aircraft's scalar measurements, i.e. water vapor, potential temperature, and methane, where a sharp transition in the scalar's magnitude is observed. Data within the growing ABL boundary layer is then selected from the total data set via a linear fit to the boundary layer heights in time, and all gradient terms from the equation above are assessed by a linear fit to this new data set. The average NO_x concentration and mean wind are averaged over the same domain within the ABL.

The oxidation rate of NO_x is considered to be controlled in the daytime by reaction with OH. A first order equivalent reaction rate was calculated from the Jet Propulsion Laboratory (JPL) Chemical Kinetics compendium (*55*), but only considered for the afternoon hours of each flight, with an average temperature and pressure measured from the flight data used to calculate the rate constant, $k_{NO2+OH.}$ The median midday peak OH was observed in a different study to be approximately $6\text{-}8 \times 10^6$ molec cm^{-3} in the San Joaquin Valley (*56*), with a flight time average of about 6×10^6, which yields an average afternoon NO_x photochemical lifetime, τ_{NO_x}, of ~4.6 (± 0.08) hours for the six flights.

The aircraft was not equipped to measure the vertical winds in order to estimate turbulent fluxes, so the flux at the top of the ABL is parameterized as an entrainment velocity, w_e, (a parameter representing the volume flux of air between the ABL and free troposphere) multiplied by the

gradient or jump between the ABL and free tropospheric concentration of NO_x. A budget of the boundary layer height was employed to calculate the entrainment velocity and the "scalar jump", $\Delta[NO_x]$, was observed (*32*). The boundary layer height budget equation can be solved for entrainment velocity

$$w_e = \frac{\partial z_i}{\partial t} + U \frac{\partial z_i}{\partial x} - W_{z_i}$$

which is the sum of the ABL growth rate, its horizontal advection, and the mean vertical velocity at the ABL top, W_{z_i}. The entrainment velocity estimated from past measurements by aircraft over the region (*32, 57*) during the warm season were shown to average between 3-5 cm s^{-1} in the midday, and the estimates from this project are very similar (average of 3.9 ± 1.5 cm s^{-1}, table S2.) The subsidence, W_{z_i}, at the top of the boundary layer was taken from Weather Research and Forecasting (WRF) model runs (S.-H. Chen personal communication) because direct measurement of vertical subsidence are not yet available by any means (see also Lenschow et al., 1999; *50*). See supplementary table 2 for the breakdown of individual boundary layer height budget terms and estimates of their errors. For a description of how the errors where generated for the budget terms in supplemental Tables 2 and 3 refer to the error analysis section of Trousdell et al. 2016 (*32*).

Due to a wildfire (*58*) that began on 22 July, 2016 some 200 km to the west of the study domain, occasionally the airborne measurements were subject to rapid spikes of NO_x (or an interfering species associated with the biomass burning plume). The wildfire effluent plumes were present mostly in the air above the boundary layer, but as the ABL grew in the afternoon these plumes would occasionally mix down into the ABL. This led to spikes occurring in the data set preferentially in the afternoon which biased our estimates of the temporal trend in NO_x. In four

cases, simply removing the spikes from the ABL data set permitted a reasonable estimate, but on two flights we had to resort to using data from the CARB surface NO_x monitoring network (https://www.arb.ca.gov/adam/hourly/hourly1.php). The trend established was the average of three station trends (from 11:00-16:00 PST) throughout the region (Fresno-Garland, Visalia-N. Church St., and Hanford-S. Irwin St.). The estimates from the surface network and aircraft were very comparable for the other four flights where both were measured (averages of -0.38 vs. -0.34 ppb/hr, respectively.) The photochemical lifetime of NO_x during midday (~5 hr) is much shorter than the advection time (10 hr) of the fire plume even if the winds were blowing directly toward the study domain. Nevertheless, even though there was likely some influence of the fire on the regional NO_x levels, the contribution entered the ABL through entrainment, which in principle is accounted for in the budgeting method by changes in the average jump across the ABL top ($\Delta[NO_x]$).

table S1. Crop classification and fertilizer rate data (mean for 1964 to 2006) collected from the DWR of California and USDA fertilizer consumption database.

ID	Fertilizer Rate (kg N/ha/yr)	Vegetation type	Notes
1	102	Citrus and Subtropical (Also Miscellaneous subtropical and jojoba)	Include Miscellaneous subtropical (307) and Jojoba (309)
2	117	Grapefruit	
3	158	Lemons	
4	110	Oranges	
5	214	Dates	
6	126	Avocados	
7	95	Olives	
8	146	Kiwis	
9	0	Eucalyptus	
10	138	Deciduous Fruits and Nuts	Includes Miscellaneous Fruits and Nuts (410) and Mixed deciduous(411)
11	70	Apples	
12	116	Apricots	
13	71	Cherries	
14	133	Peaches and Nectarines	
15	141	Pears	
16	128	Plums	
17	157	Prunes	
18	86	Figs	
19	252	Almonds	
20	103	Walnuts	
21	224	Pistachios	
22	157	Field Crops	Includes Flax (603), Hops (604), Castor Beans (609), Miscellaneous Field (611), Millet (614)
23	205	Cotton	
24	115	Safflower	
25	211	Sugar Beets	
26	280	Corn (Field and Sweet)	
27	157	Grain sorghum	
28	247	Sudan	
29	99	Beans (dry)	

30	168	Sunflowers	
31	119	Grain and Hay	Includes Miscellaneous grain and hay (706)
32	45	Barley	
33	617	Wheat	
34	67	Oats	
35	0	Pasture	
36	13	Alfalfa	
37	0	Clover	
38	0	Mixed pasture	
39	0	Native Pasture	
40	0	Induced high water table native pasture	
41	0	Miscellaneous grasses	
42	198	Turf farms	
43	158	Rice	Includes rice (1801) and wild rice (1802)
44	187	Truck, Nursery, Berry Crops	Includes cole mixture (2004), mixed (2017), miscellaneous truck (2018)
45	196	Artichokes	
46	173	Asparagus	
47	138	Beans (green)	
48	258	Carrots	
49	324	Celery	
50	222	Lettuce	
51	33	Melons, squash, cucumbers	
52	234	Onions and garlic	
53	99	Peas	
54	279	Potatoes	
55	228	Sweet Potatoes	
56	89	Spinach	
57	202	Tomatoes (processing)	
58	0	Flowers, nursery, Christmas tree farms	
59	231	Bush berries	
60	204	Strawberries	
61	404	Peppers	
62	228	Broccoli	
63	198	Cabbage	

64	290	Cauliflower	
65	198	Brussle Sprouts	
66	0	Greenhouse	
67	32	Vineyards	Includes Table grapes (2201), Wine Grapes (2202), Raisin grapes (2203)

table S2. ABL heights, z_i, and budget terms for the six flights. The error estimates for each term are in the right adjacent columns.

Flight Date	$\partial z_i/\partial t$ (cm/s)	error (cm/s)	$-U(\partial zi/\partial t)$ Advection (cm/s)	error (cm/s)	W (cm/s)	error (cm/s)	w_e (cm/s)	error (cm/s)	Mean z_i (m)
7/27/16	2.8	0.7	0.6	0.5	-1.9	0.5	5.3	1.0	613
7/28/16	3.6	1.1	0.1	0.2	-2.1	0.5	5.8	1.2	622
7/29/16	0.8	0.6	-0.1	0.2	-1.9	0.5	2.6	0.8	602
8/4/16	1.1	0.5	0.9	0.2	-2.0	0.5	4.0	0.7	740
8/5/16	0.5	0.4	-0.1	0.1	-2.8	0.5	3.2	0.7	606
8/6/16	-1.0	0.6	0.4	0.1	-2.9	0.5	2.3	0.8	660
Averages	**1.3**	**0.7**	**0.3**	**0.2**	**-2.3**	**0.5**	**3.9**	**0.9**	**640**
1σ	**1.7**		**0.4**		**0.5**		**1.3**		**49**

table S3. NO_x budget table and the consequent total regional emissions for each flight. The error estimates for each term are in the right adjacent columns.

Flight Date	$\partial[NO_x]/\partial t$ Storage (ppbv/hr)	$-U(\partial[NO_x]/\partial x)$ Advection (ppbv/hr)	$w_e \Delta[NO_x]/z_i$ (ppbv/hr)	$-k[OH][NO_x]$ Chem Loss (ppbv/hr)	F_0/z_i Emission (ppbv/hr)	τ_{NOx} lifetime (hr)	Sum Regional Emissions (tons/day)	error (tons/day)	Avg. ABL $[NO_x]$ (ppbv)	1σ (ppbv)
7/27/16	-0.29	0.01	-0.5	-1.9	2.5	4.7	250	108	9.3	2.3
7/28/16	-0.09	-0.09	-0.6	-1.8	2.5	4.7	280	157	8.4	2.3
7/29/16	-0.44	0.30	-0.2	-2.0	2.5	4.7	176	81	6.8	1.0
8/4/16	-0.73	0.04	-0.3	-1.2	2.5	4.6	100	150	6.2	4.4
8/5/16	-0.83	-0.01	-0.3	-1.7	2.5	4.5	138	143	7.8	2.7
8/6/16	-0.35	-0.02	-0.2	-1.7	2.5	4.5	197	130	7.1	0.8
Averages	**-0.46**	**0.04**	**-0.3**	**-1.7**	**2.5**	**4.6**	**190**	**128**	**7.6**	**2.2**
1σ	**0.28**	**0.1**	**0.2**	**0.3**	**0.0**	**0.1**	**67**	**29**	**1.1**	**1.3**

red indicates estimate made from surface network NOx measurements

table S4. Flight estimates of total NO$_x$ and soil NO$_x$ and model estimates of soil NO$_x$ for the flight area in fig. S3 [Coordinates box: (36º51′52.09″N, 120º43′19.65″W), (37º0′6.85″ N, 119º50′53.87″W), (35º57′49.03″N, 120º1′37.93″W), and (36º5′27.03″N, 118º58′2.91″W) compared with CARB inventory of total NO$_x$].

	Mean NO$_x$ (kg N/ha/yr)	Total NO$_x$ (Ton N/yr)	Area (ha)
Model year-round estimates of soil NO$_x$ without canopy exchange	24.7	24,000	971,200
Model year-round estimates of soil NO$_x$ considering canopy exchange	12.3	12,000	971,200
Model Jul-Aug. estimates of soil NO$_x$ without canopy exchange	36.4	35,300	971,200
Model Jul-Aug. estimates of soil NO$_x$ considering canopy exchange	18.2	17,700	971,200
CARB inventory of total NO$_x$	3.6	11,248	3,168,000
Flight estimates of total NO$_x$	29.3	21,100	720,000
Flight estimates of soil NO$_x$	13.8	9,900	720,000

"Jul-Aug." means the annual rate was estimated using July and Aug. rates only (assuming the remaining months have the same rate as the mean of July and Aug).
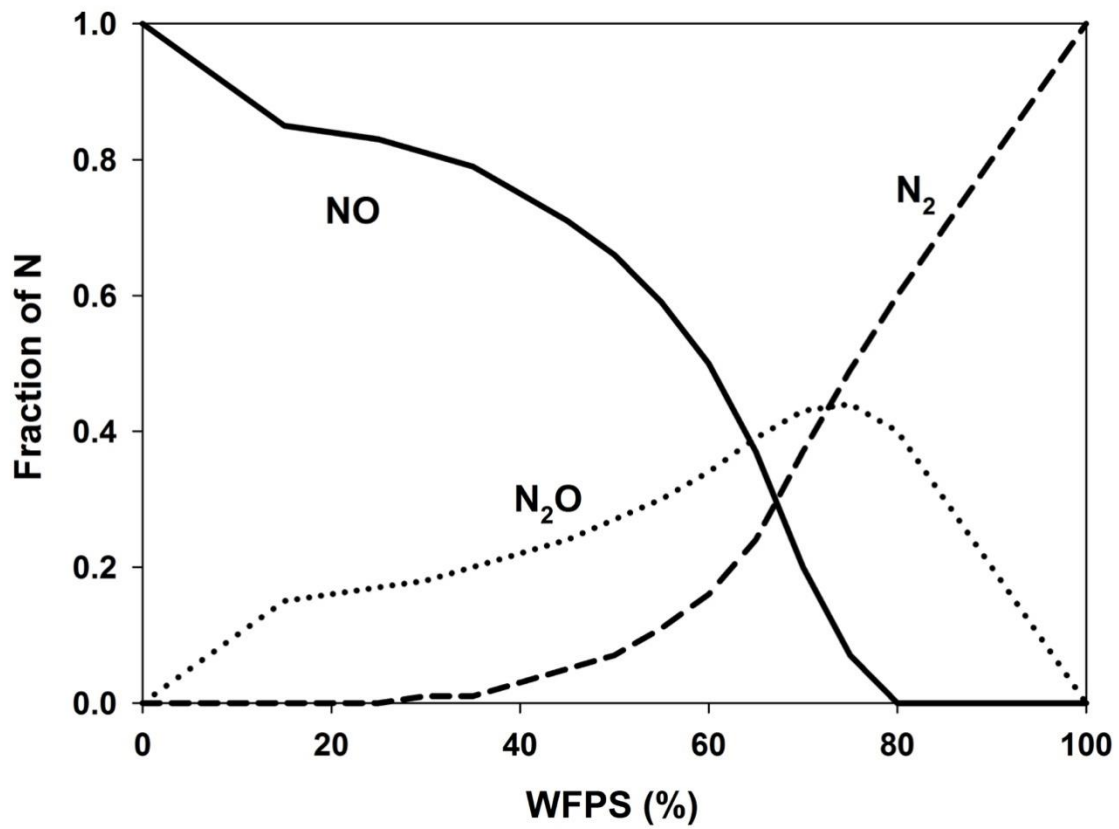
fig. S1. Model of how nitrogen oxide (NO), nitrous oxide (N_2O), and dinitrogen (N_2) partitioning varies with water-filled pore space.
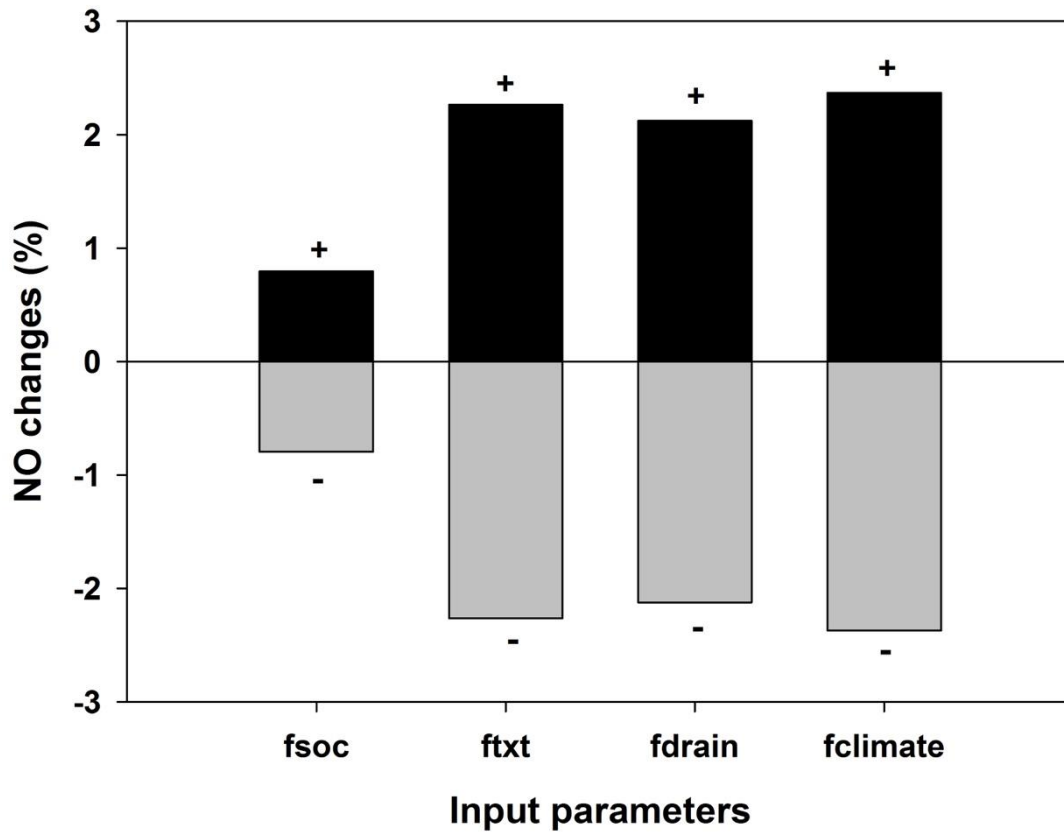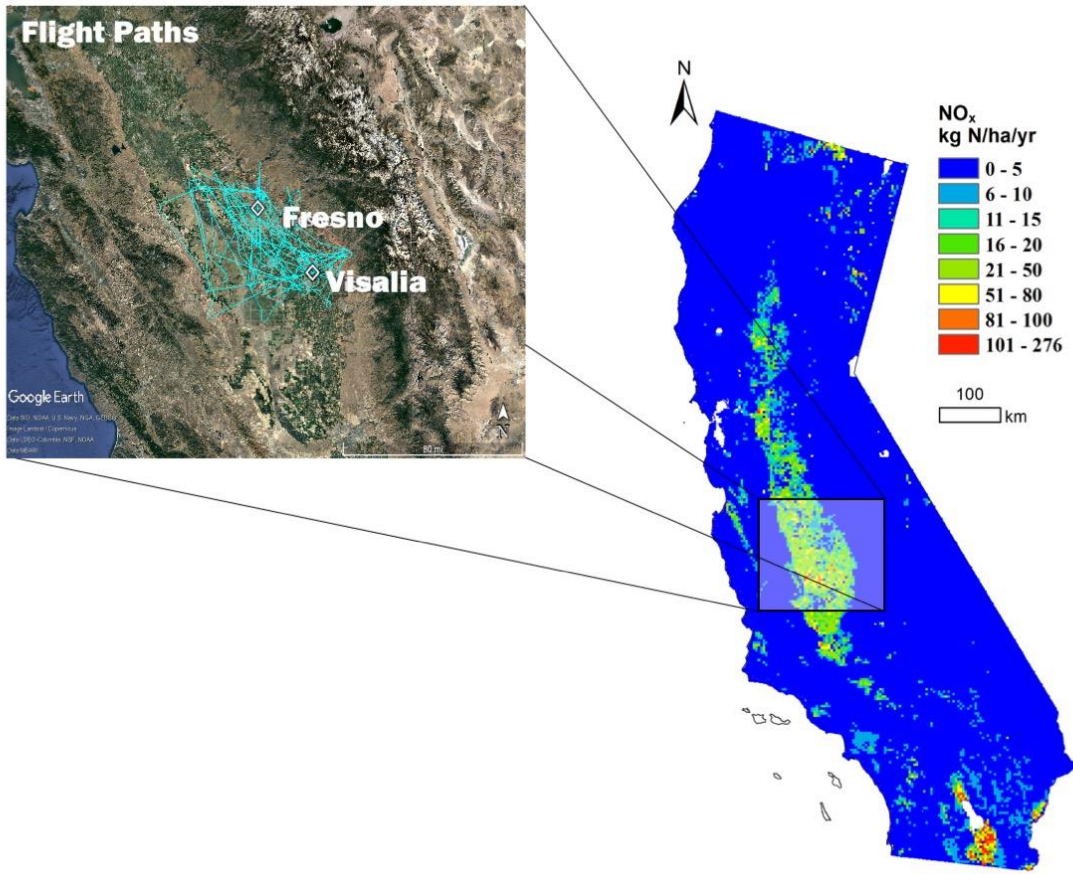
fig. S2. Sensitivity of NO emission from croplands to different input parameters: soil organic carbon (fsoc), soil texture (ftxt), soil drainage (fdrain), and climate (fclim).

fig. S3. Airborne NO$_x$ observation sampling area. Flight paths (turquoise lines) from all six airborne NO$_x$ observation flights that estimated surface emissions (left) superimposed onto IMAGE modeled soil NO$_x$ emissions map for California (right).